Fluorescence Stopped-Flow Study of the Mechanism of Nucleotide Binding to Myosin Subfragment 1†

Frank Garland* and Herbert C. Cheung

ABSTRACT: The mechanism of nucleotide binding to myosin subfragment 1 (S1) in the presence of Mg^{2+} has been investigated by measuring the rate of enhancement or of quenching of intrinsic (tryptophan) fluorescence when protein is reacted with either native nucleotides (ATP or ADP) or their fluorescent analogues, 1,N^6-ethenoadenosine 5′-tri- or -diphosphate (ϵATP or ϵADP). The influence of the DTNB light chain (LC2) of the protein on the binding process was studied by performing comparative experiments with intact S1 [S1(Mg)] and with light-chain deficient S1 [S1(EDTA)]. The kinetic isotherms, obtained by measuring the apparent first-order rate constant as a function of excess nucleotide concentration, were nonlinear for both native nucleotides and for analogue substrate. The maximum observed rate was 39 and 32 s^{-1}, respectively, for ATP and ADP reacted with intact S1 but 32 and 28 s^{-1} with S1(EDTA) (4 °C, 0.1 M KCl, 5 mM $MgCl_2$, and 0.1 mM dithiothreitol, pH 8.0). The ATP and ADP isotherms did not fit the rectangular hyperbolic concentration dependence predicted by the two-step binding model of Bagshaw et al. [Bagshaw, C. R., Eccleston, J. F., Eckstein, F., Goody, R. S., Gutfreund, H., & Trentham, D. R. (1974) *Biochem. J. 141*, 351]. Although high concentration plateaus were not attained in the case of ϵATP, the data could be fitted to hyperbolas, yielding maximum rates of 260 and 140 s^{-1} with S1(Mg) and S1(EDTA), respectively. The reaction of ϵADP with intact S1 gave an apparently linear isotherm; however, biphasic traces were obtained above 0.3 mM nucleotide. The corresponding light chain deficient experiments yielded biphasic traces which were resolvable into two components: a fast component which appears to level off in the 150–200-s^{-1} region, and a slow component which attains a maximum rate of 28 s^{-1} at high concentrations. The experimental results, taken together, indicate that a minimum of three steps is needed to describe nucleotide binding. On the basis of the data and computer simulation calculations, a mechanism representing a simple extension of the Bagshaw–Trentham model is proposed.

$$M + X \overset{1}{\rightleftharpoons} M{\cdot}X \overset{2}{\rightleftharpoons} M^{\dagger}{\cdot}X \overset{3}{\rightleftharpoons} M^{*}{\cdot}X$$

M represents S1, and X represents one of the four nucleotides used in this work. The slow step, step 3, corresponds to the relatively slow first-order transition observed with the ATP, ADP, and S1(EDTA)/ϵADP systems whereas step 2 is responsible for the rapid phase observed with analogue nucleotides. The experimental and computer results suggest that step 2 may involve some degree of fluorescence enhancement when X ≡ ATP or ADP and also that the equilibrium constant of this step is relatively large ($K_2 \geq 10^3$ M^{-1}) when X is substrate but small (K_2 = 1–4 M^{-1}) when X is product nucleotide. The implications of these findings with respect to the acto-S1 ATPase mechanism are discussed.

The mechanism of the magnesium ion dependent ATPase[1] of myosin has been the subject of extensive research effort in recent years. The relevance of such studies to the contractile process was considerably enhanced by Lymn & Taylor (1971), who demonstrated that the addition of ATP to actomyosin dissociated the latter complex into the component proteins and that the rate of dissociation is much faster than the rate of substrate hydrolysis. From these and other results a mechanism was proposed according to which hydrolysis occurs while myosin is dissociated from actin. The steps of the Lymn–Taylor mechanism can be identified with the different stages of the contractile cycle postulated in the sliding filament model of Huxley (1969). Lymn & Taylor (1971) also found that the hydrolysis rate becomes constant at high substrate concentrations. This observation prompted Bagshaw et al. (1974) to measure the rate of ATP binding to myosin subfragment 1 as a function of nucleotide concentration in order to investigate the possibility that the hydrolysis rate might be controlled by some first-order process occurring prior to the hydrolysis step. It was found that the apparent rate of ATP binding, as measured by the enhancement of tryptophan fluorescence, was independent of substrate concentration above ~0.4 mM. Since similar results were obtained for ADP and for the essentially unhydrolyzable ATP analogue adenosine 5′-(3-thiotriphosphate), it was concluded that nucleotide binding to a myosin active site is a two-step process: a rapid binding step followed by an isomerization of the encounter complex. The first-order step, but not the binding step, gives rise to the observed enhancement of tryptophan fluorescence. The authors assumed that the binding step is in rapid equilibrium as the second step proceeds. Sleep & Taylor (1976) subsequently investigated the interaction of the actomyosin subfragment 1 complex with ATP by simultaneously monitoring both light scattering and intrinsic protein fluorescence. The rate of protein dissociation, as measured by light scattering, was found to be considerably faster than the rate of fluorescence enhancement. It was also observed that the high concentration rate of the enhancement step was not very different in the presence of actin than in its absence. These results

† From the Biophysics Section, Department of Biomathematics, University of Alabama in Birmingham, Birmingham, Alabama 35294. *Received September 12, 1978; revised manuscript received September 10, 1979.* This work was supported by National Institutes of Health Grant AM 17483 and by a U.A.B. Medical Center Faculty Research Grant awarded to F.G. A preliminary report of these results has been published (Garland & Cheung, 1978).

[1] Abbreviations used: ATP and ADP, adenosine 5′-tri- and -diphosphate; ATPase, adenosine triphosphatase; ϵATP and ϵADP, 1,N^6-ethenoadenosine 5′-tri- and -diphosphate; EDTA, ethylenediaminetetraacetic acid; DTNB light chain, 19 000-dalton subunit of myosin obtained by treatment with 5,5′-dithiobis(2-nitrobenzoate); S1, myosin subfragment 1; S1(EDTA), myosin subfragment 1 from which the DTNB light chain has been extensively removed during papain digestion of insoluble myosin in the presence of EDTA; S1(Mg), intact S1 obtained by doing the digestion in the presence of Mg^{2+}; Tris, 2-amino-2-(hydroxymethyl)-1,3-propanediol; DEAE, diethylaminoethyl.

0006-2960/79/0418-5281$01.00/0

suggest that the substrate binding step itself triggers the dissociation of actin and that the fluorescence enhancing step is essentially irrelevant to actomyosin dissociation. More recently, Johnson & Taylor (1978) reexamined the kinetics of the binding of ATP to S1 and to acto-S1. On the basis of various data, a three-step mechanism was postulated for the reaction of ATP with S1. The third step of the mechanism is the fluorescence enhancement step originally observed by Bagshaw et al. (1974), but for substrate it is suggested to involve hydrolysis. Attention has also been focused on the possible role of the DTNB light chain (LC2) in the interaction of myosin with actin. Observing that the calcium binding capacity of DTNB-treated myosin was significantly reduced from that of untreated myosin, Werber & Oplatka (1974) suggested that the light chain might have a control function similar to that of troponin C. However, Bagshaw & Reed (1977) have shown that the kinetics of Ca^{2+} (or Mg^{2+}) binding to the DTNB light chain is too slow for the latter to have any direct regulatory role. Nonetheless, it remains true that the DTNB light chain affects the interaction of myosin with actin both in the absence (Margossian et al., 1975) and presence (Hozumi & Hotta, 1978) of ATP.

We have reinvestigated the binding kinetics of nucleotides to myosin subfragment 1 by using stopped-flow fluorometry, with particular interest in mechanistic events which might be relevant to the actomyosin dissociation step. Since it is apparently quite difficult to directly observe the early events (that is, processes occurring prior to the fluorescence enhancement step) with the native substrate, we have used a fluorescent analogue of ATP, ϵATP. Since the binding of ϵ nucleotides to a myosin active site results in quenching of tryptophan fluorescence through energy transfer (Onishi et al., 1973), it was anticipated that the use of ϵATP and ϵADP might enable us to look at the actual binding step and possibly at mechanistic events related to actomyosin dissociation. This hope was founded on the fact that a signal depending on energy transfer need not involve protein structural changes of the type thought to be responsible for the enhancement of tryptophan fluorescence by ATP (Werber et al., 1972). A signal may be produced simply by a change in the distance between donor (in this case the tryptophan residues) and acceptor (ϵ nucleotide), as in binding. In addition, any mechanistic event resulting in a change in the orientation of bound ϵ nucleotide with respect to the donor tryptophan will also produce an observable change in the energy transferred and hence in the degree of tryptophan quenching. Since we are also interested in the effect of the DTNB light chain on the early events of nucleotide binding, experiments were done with light chain deficient S1 as well as with intact S1. Comparative experiments were done with the native nucleotides in order to determine how well the ϵ nucleotides mimic ATP and ADP. The experiments were done at low temperatures in order to slow the reactions down. We have previously shown that the myosin active sites are identical and noninteracting with respect to ϵADP binding (Garland & Cheung, 1976). Evidence for a similar conclusion for ADP has been obtained by Marsh et al. (1978) in an extensive study of the binding of the native nucleotide to heavy meromyosin and S1. In this work we have assumed that the S1 binding sites are homogeneous and identical in their interaction with substrate as well as product nucleotides, fluorescent analogue as well as native. The assumption is made for each of the two types of protein preparations.

Materials and Methods

Myosin was prepared from rabbit back muscle by using a modification of the Szent-Györgyi method (Tonomura et al., 1966) and was then dialyzed overnight against 0.2 M ammonium acetate containing either 2 mM $MgCl_2$ or 2 mM EDTA. Intact S1, designated S1(Mg), and DTNB light chain deficient S1, S1(EDTA), were obtained from the papain digestion of insoluble myosin in the presence of either 2 mM $MgCl_2$ or 2 mM EDTA, respectively (Margossian et al., 1975). Subfragment 1 obtained from the digestion was subsequently purified by DEAE-cellulose column chromatography (Whatman DE-52) and ammonium sulfate fractionation again in the presence or complete absence of divalent cation. Sodium dodecyl sulfate–polyacrylamide gels (10%) showed S1(EDTA) to be essentially free of DTNB light chain; the S1(Mg) gels showed an intense DTNB light-chain band. The concentrations of subfragment 1 in solution were determined by using molecular weights of 1.2×10^5 for S1(Mg) and 1.0×10^5 for S1(EDTA) and a percent extinction coefficient of $E_{280}^{1\%} = 7.9$ cm^{-1} for both proteins. Correction was made for protein scattering.

ATP, ADP, ϵATP, and ϵADP were purchased from Sigma Chemical Co. (St. Louis, MO); their purity was checked by thin-layer chromatography. Concentrations of the nucleotides were determined by using the following molar extinction coefficients (M^{-1} cm^{-1}): $E_{259} = 1.54 \times 10^4$ for ATP and ADP; $E_{265} = 5700$ and $E_{275} = 5600$ for ϵATP; $E_{265} = 5800$ and $E_{275} = 5900$ for ϵADP.

The experiments were done in solutions containing 0.1 M KCl, 50 mM Tris, 5 mM $MgCl_2$, and 0.1 mM dithiothreitol (DTT), pH 8.0, prepared from degassed distilled water. All kinetic experiments were done at 4 °C in a Durrum D-110 spectrophotometer equipped with fluorescence optics. Tryptophan fluorescence was isolated with a Ditric three-cavity 334-nm interference filter; ϵ-nucleotide fluorescence was observed by using a 430-nm cutoff filter (Corning 3-73). The traces obtained from the kinetic experiments were digitized and stored for later analysis by using a DEC PDP-8/I minicomputer equipped with an AX-08 AD/DA converter. The PDP-8/I is cable-linked to a Xerox Sigma 7 computer to which the digitized traces could be transferred for data analysis. The individual kinetic experiments, carried out under pseudo-first-order conditions, were analyzed by fitting the traces to

$$F(t) = F_\infty[1 - \Delta F \exp(-k_{obsd}t)] \quad (1)$$

using a nonlinear least-squares program based on the Marquardt (1963) algorithm. $F(t)$ represents the observed fluorescence signal; the traces were fit to eq 1 for the best least-squares values of F_∞, ΔF, and k_{obsd}. The statistic used to determine whether or not an individual trace could be fit by a single-exponential function was the χ^2 ratio, defined as

$$\chi_R^2 = \frac{\sum(\delta F_i^2/\sigma_i^2)}{N - p}$$

δF_i^2 is the difference between the measured and fitted values of the ith data point, σ_i^2 is the variance of the ith data point, N is the total number of data points (usually 500), and p is the number of parameters being fitted. σ_i^2 was estimated from the variation of the data points at the end of the trace, when the reaction had reached equilibrium, and was taken to be equal for all data points of a given trace. The value of χ_R^2 corresponding to a 95% confidence limit is 1.1 for the number of degrees of freedom (equal to $N - p$) involved in these fits. A value of χ_R^2 significantly greater than 1.1 means that the trace in question cannot be fitted by a single-exponential function (eq 1) to within experimental error. When this occurred, an attempt was made to fit such a trace to a double-exponential function

$$F(t) = F_\infty[1 - \Delta F^+ \exp(-k_{obsd}^+ t) - \Delta F^- \exp(-k_{obsd}^- t)] \quad (2)$$

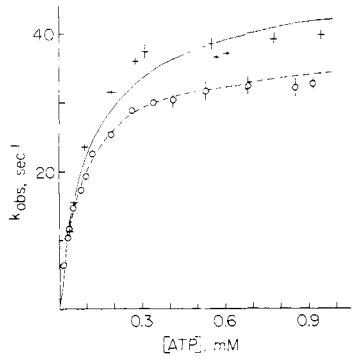

FIGURE 1: Dependence of the observed pseudo-first-order rate constant, k_{obsd}, on excess ATP concentration when the latter is reacted with either S1(Mg) (+) or S1(EDTA) (○). The vertical bars represent the standard deviation of a single measurement of k_{obsd}, calculated from five to seven duplicate measurements. The drawn curves show the best least-squares fits of the Bagshaw–Trentham model (given by eq 7) to the data. Intrinsic protein (tryptophan) fluorescence was monitored: excitation wavelength = 295 nm, emission wavelength = 334 nm.

using the nonlinear least-squares program mentioned above. ΔF^+, ΔF^-, $k_{obsd}{}^+$, and $k_{obsd}{}^-$ are the amplitudes and first-order rate constants obtained by fitting biphasic traces to eq 2. Only in the S1(EDTA)/ϵADP system did we succeed in resolving traces for which $\chi_R{}^2 > 1.2$ into two exponentials. In the other cases either the two time constants were not sufficiently different or else one phase was too rapid (and the amplitude too small) to successfully fit the trace to eq 2. In this connection, it should be mentioned that accurate measurement of rapid, low-amplitude processes is very difficult, at the present time, with our instrument because of (1) the fact that the mechanical arrangement by which the flow is stopped results in shock waves which interfere with the recorded signal during the first several milliseconds of the trace and (2) the relatively slow mixing time of our apparatus. Thus, we cannot yet confirm the presence or absence of lags. The same factors make the measurement of relative fluorescence changes very difficult and inaccurate.

Results

Native Nucleotides. The overall binding of a nucleotide molecule to an S1 active site may be described by

$$M + X \underset{k_d}{\overset{k_a}{\rightleftharpoons}} M{\cdot}X \qquad (3)$$

M, X, and M·X represent free enzyme, free nucleotide (either substrate or product), and enzyme–nucleotide product, respectively. k_a and k_d are the apparent association and dissociation rate constants. k_a may be obtained without prior knowledge of the overall binding constant by performing the experiment under pseudo-first-order conditions. If one of the reactants is in large excess, the fluorescence change due to the reaction would be described by eq 1; in this case, the observed first-order rate k_{obsd} is related to the rate constants of eq 3 by

$$k_{obsd} = k_a C + k_d \qquad (4)$$

C is the concentration of the reactant in large excess. Equation 4 shows that if the actual binding mechanism consists of a single step, such as eq 3, k_{obsd} will vary linearly with C. If, however, the binding process includes first-order steps which are detected by the stopped-flow measurements, quite different behavior may result. Figures 1 and 2 show k_{obsd} plotted against the concentration of ATP and ADP, respectively. In these experiments, the concentration of nucleotide was at least 15 times that of enzyme; intrinsic protein fluorescence was monitored. All four native nucleotide isotherms show significant

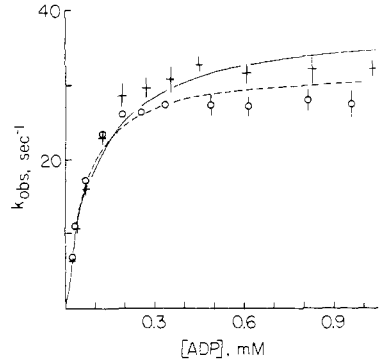

FIGURE 2: Dependence of k_{obsd} on excess [ADP]. Significance of the symbols, error bars, and drawn curves, as well as the experimental conditions, is the same as in Figure 1.

deviation from linearity. The nonlinear dependence of k_{obsd} on ATP (and ADP) concentration was first noted by Bagshaw et al. (1974) and has since been confirmed by others (Sleep & Taylor, 1976; Taylor & Weeds, 1977). These authors have analyzed their data in terms of a sequential, two-step mechanism proposed by Bagshaw and co-workers.

$$M + X \underset{k_{-b}}{\overset{k_b}{\rightleftharpoons}} M{\cdot}X \underset{k_{-c}}{\overset{k_c}{\rightleftharpoons}} M^*{\cdot}X \qquad (5)$$

k_b and k_{-b} are the forward and reverse rate constants of the binding step, and k_c and k_{-c} are the rate constants of a ligand-induced conformational change. According to the model, the intrinsic fluorescence intensity of the protein in the M·X state is the same as that in the free state while that of M*·X is enhanced. As above, X represents either substrate or product nucleotide. This reaction scheme results in biphasic stopped-flow traces; the first-order time constants are obtained as the roots of the quadratic equation derived from the rate equations and are given by (Frost & Pearson, 1961)

$$\lambda_1 = \tfrac{1}{2}(p + q)$$
$$\lambda_2 = \tfrac{1}{2}(p - q) \qquad (6)$$

where

$$p = k_b' + k_{-b} + k_c + k_{-c}$$
$$q = \sqrt{p^2 - 4(k_b'k_c + k_{-b}k_{-c} + k_b'k_{-c})}$$
$$k_b' = k_bC$$

C is the concentration of the reactant in large excess. Examination of the concentration dependence of these roots shows that whereas λ_1 increases indefinitely with increasing C, λ_2 levels off at high concentrations, approaching a value of $k_c + k_{-c}$. The Bagshaw–Trentham model makes use of the equilibrium approximation. That is, it is assumed that the binding step is in rapid equilibrium as M*·X is formed from M·X. This means that $k_{-b} \gg k_c$. The concentration dependence of λ_2 then assumes the characteristic hyperbolic shape given by (Bagshaw et al., 1974)

$$\lambda_2 = \frac{K_bk_cC}{K_bC + 1} + k_{-c} \qquad (7)$$

where $K_b = k_b/k_{-b}$. Deviation from the hyperbola is a measure of the extent to which the inequality on which eq 7 is based is not fulfilled. An important consideration is that the limiting (low concentration) slope of the hyperbola depends on k_b and on the relative magnitudes of k_{-b} and k_c. When the equilibrium approximation applies, i.e., when $k_{-b} \gg k_c$, the limiting slope is equal to K_bk_c, as eq 7 shows. On the other hand, the limiting slope equals k_b when $k_{-b} \ll k_c$ and takes on interme-

Table I: Apparent Association and Dissociation Rate Constants Measured at Low Concentrations of Subfragment 1 and Nucleotide[a]

nucleotide	rate constants S1(Mg)	S1(EDTA)
	k_a (M^{-1} s^{-1})	
ATP	(2.8 ± 0.2) × 10^5	(2.9 ± 0.2) × 10^5
ADP	(2.7 ± 0.2) × 10^5	(3.0 ± 0.2) × 10^5
ϵATP	(2.8 ± 0.2) × 10^5	(3.8 ± 0.3) × 10^5
ϵADP	(1.1 ± 0.1) × 10^5	(1.4 ± 0.1) × 10^5
	k_d (s^{-1})	
ϵADP	0.22 ± 0.01	0.20 ± 0.01

[a] Results given are the average of numerous measurements from several preparations of protein; uncertainties shown are the standard error of a measurement.

diate values when k_{-b} and k_c are similar in magnitude.

The binding of the native nucleotides to S1(Mg) or S1(EDTA) was followed by monitoring the change in intrinsic protein fluorescence as the reaction proceeds. The values of k_{obsd} obtained by fitting the resulting traces to eq 1 are shown plotted as a function of total nucleotide concentration in Figures 1 and 2. All of the traces fit the single-exponential function to within experimental error (χ_R^2 = 0.9–1.2) except those in the 0.15–0.3 mM concentration range, where χ_R^2 values of 1.5–1.8 were obtained; the S1(EDTA)/ATP system gave especially poor fits at these concentrations, with χ_R^2 ranging up to 2.5. These poor fits could be due to a second component having a very rapid rate and small or zero amplitude. Biphasic traces have been reported by Taylor (Johnson & Taylor, 1978). In addition, the fact that this behavior is not observed with the ϵ nucleotides would support a conclusion as to the existence of a rapid component with the native nucleotides. However, because of the instrument limitations referred to under Materials and Methods, we are reluctant to make this conclusion at this time. Traces obtained at these intermediate concentrations were analyzed by successively deleting an increasingly larger fraction of the initial portion of the traces. The value of χ_R^2 decreased to ~1.0 as more of each trace was deleted; the fitted value of k_{obsd} remained constant after good fits were obtained. It is these values of k_{obsd} which are plotted in Figures 1 and 2.

The rate of fluorescence enhancement of the reaction of ATP and ADP with S1(Mg) and S1(EDTA) initially increases linearly with nucleotide concentration but levels off above ~0.3 mM ligand. The limiting slope and intercept of the kinetic isotherms give the apparent association and dissociation rate constants (k_a and k_d), respectively. k_a may also be calculated from individual low concentration experiments, using eq 4, providing k_d is either negligible or known. Previous work has shown that at room temperature ATP dissociates from myosin subfragment 1 at a rate of 0.02 s^{-1} or less while ADP does so at a rate of 1.4 s^{-1} (Bagshaw & Trentham, 1974). The latter nucleotide exhibits a very large temperature dependence for this process, the rate being 0.07 s^{-1} at 5 °C (0.1 M KCl, 5 mM $MgCl_2$, and 50 mM Tris, pH 8.0). Our own experiments show that the overall rate of dissociation of the fluorescent analogue of ADP, ϵADP, is 0.2 s^{-1} under similar conditions (see Table I). We therefore assume that k_d is negligible under the experimental conditions used here. The k_a's calculated from the low concentration data are given in Table I. It may be seen that the values of k_a are identical, to within experimental error, for the four protein/nucleotide systems investigated. On the other hand, the high concentration rate of fluorescence enhancement does vary somewhat over the four systems.

Table II: Results of Least-Squares Fits of Eq 7 to the ATP, ϵATP, and ADP Kinetic Isotherms

system	k_b (M^{-1})	k_c (s^{-1})	χ_R^2[a]
S1(Mg)/ATP	(9.8 ± 2.5) × 10^3	46 ± 4	10.6
S1(EDTA)/ATP	(1.1 ± 0.2) × 10^4	35 ± 3	2.3
S1(Mg)/ϵATP	(1.2 ± 0.2) × 10^3	260 ± 60	0.6
S1(EDTA)/ϵATP	(2.6 ± 0.5) × 10^3	140 ± 50	1.4
S1(Mg)/ADP	(1.0 ± 0.2) × 10^4	37 ± 3	3.0
S1(EDTA)/ADP	(1.6 ± 0.3) × 10^4	33 ± 3	3.9

[a] The value of χ_R^2 corresponding to a 95% confidence limit is ~1.7 for the number of degrees of freedom involved in these fits.

The nonlinear concentration dependence of k_{obsd} means that the binding process must consist of at least two steps for both substrate and product nucleotide. In terms of the sequential two-step mechanism given by eq 5, it is clear that k_{obsd} corresponds at least primarily to the slower component, λ_2. Note that all values of k_{obsd} were obtained from traces or parts of traces which fit a single-exponential decay function (eq 1) to within experimental error. We thus equate k_{obsd} with λ_2. This assumes that, in deleting the initial portion of those traces which appear to show phase lag character, the fast component was eliminated. The assumption that $k_{obsd} = \lambda_2$ is valid providing that the fast component is a factor of at least 3 or 4 larger than the slow component and has a relatively small amplitude, as seems to be the case here. The Bagshaw–Trentham model was tested by fitting eq 7 to the experimental isotherms using the nonlinear least-squares program mentioned under Materials and Methods. In this analysis we have assumed that k_{-c} is less than ~0.2 s^{-1} under the experimental conditions used here. The results obtained from the fits are given in Table II; the theoretical isotherms are plotted as solid and dashed lines in Figures 1 and 2. Fitting the data for values of k_{-c} (held constant during a given fit) up to 0.4 s^{-1} did not significantly affect the results. It may be seen that none of the four isotherms fit the hyperbola to within experimental error. It should be noted that a value of χ_R^2 of 2.5 corresponds to a 0.5% (or lower) level of significance (i.e., $P_{99.5}$ = 2.5) for the number of degrees of freedom involved in these fits. Thus, the deviation of the data, especially the ADP and S1(Mg)/ATP isotherms, from eq 3 must be regarded as significant. Failure of the data to fit the hyperbola indicates that the inequality on which eq 7 is based, namely, $k_{-b} \gg k_c$, is not fulfilled; i.e., $k_{-b} \lesssim k_c \simeq 40$ s^{-1}. This suggests that $k_b = K_b k_{-b} \simeq (10^4\ M^{-1})(40\ s^{-1}) = 4 \times 10^5\ M^{-1}\ s^{-1}$, which is an order of magnitude less than typical protein–ligand association rates (Gutfreund, 1971). An attempt was made to fit the two-step mechanism (eq 5) to the S1(Mg)/ATP data, without the restriction imposed by assuming the equilibrium approximation, by fitting the experimental isotherm with the exact equation for λ_2 (eq 6). The results are $k_b = (4 \pm 1) \times 10^5$ M^{-1} s^{-1}, $k_{-b} = (10 \pm 5) \times 10^5$ s^{-1}, $k_c = (40 \pm 2) \times 10^5$ s^{-1}, and $k_{-c} = (0.05 \pm 0.2) \times 10^5$ s^{-1} (χ_R^2 = 1.3). The data do fit the theoretical isotherm to within experimental error, as perhaps would be expected with four adjustable parameters. On the other hand two observations may be made: (1) the fitted value of k_b is again uncharacteristically low; (2) the rate constants obtained from the fit would yield traces which would be distinctly biphasic. For example, at 0.1 mM ATP, the time course of the observed signal would follow [see eq 42, Frost & Pearson (1961)]

$$F(t) = F_\infty[1 + 0.59 \exp(-66t) - 1.59 \exp(-24t)]$$

providing, as was concluded by Bagshaw et al. (1974), that only the M·ATP to M*·ATP transition involves an observable signal change. The experimental traces did not exhibit the

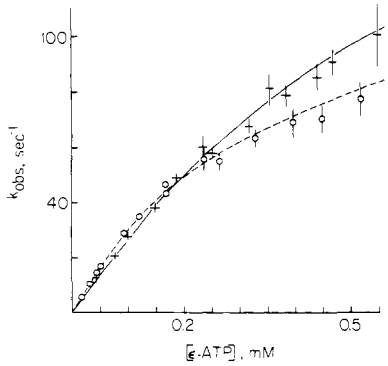

FIGURE 3: Dependence of k_{obsd} on excess ϵATP concentration for nucleotide reacted with S1(Mg) (+) or S1(EDTA) (O). Drawn curves show the best least-squares fits of eq 7 to the data. Intrinsic protein fluorescence was monitored.

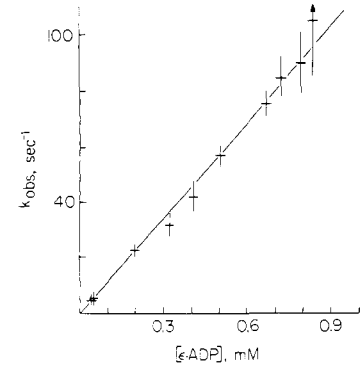

FIGURE 4: Concentration dependence of k_{obsd} for ϵADP reacted with S1(Mg). Conditions are the same as those in Figure 1.

degree of biphasicity predicted by these results. Thus, our rate data cannot be satisfactorily interpreted in terms of the Bagshaw–Trentham scheme, with or without the equilibrium approximation.

The experimental results show that some significant differences exist between intact and DTNB light chain deficient S1 with regard to their interaction with the native nucleotides. Although the limiting slopes of all four isotherms are identical, removal of the light chain results in a ~20% decrease in the high concentration rate of fluorescence enhancement for ATP but only 10% for ADP. It may also be seen from Table II that a significant difference exists in the degree to which the two substrate isotherms fail to fit eq 7 but that the two ADP isotherms deviate from the hyperbola to a similar degree.

Analogue Nucleotides. Figure 3 shows the concentration dependence of k_{obsd} for the binding of ϵATP with S1(Mg) and S1(EDTA). As in the case of the native nucleotides, the reaction was followed by monitoring the change in intrinsic protein fluorescence. Because of the appreciable absorbance of the ϵ nucleotides at the excitation wavelength (295 nm), the uncertainty in the fitted values increases significantly at higher concentrations. The fluorescent nucleotides have no detectable emission at the wavelength used to monitor intrinsic protein fluorescence (334 nm). At low concentrations the reaction was also followed by monitoring the change in nucleotide emission on direct excitation, as well as the change in sensitized nucleotide emission; the resulting values of k_{obsd} were identical with those obtained by monitoring intrinsic protein fluorescence at the same concentrations. Unlike the native nucleotides, all traces fit a single-exponential decay function (eq 1) to within experimental error ($\chi_R^2 < 1.3$); no evidence of biphasicity was detected. The isotherms of both proteins again show significant deviation from linearity, indicating that a multistep mechanism is needed to describe the binding of analogue substrate to the proteins. The results obtained by fitting the hyperbola (eq 7) to the ϵATP data are given in Table II. It may be seen that both isotherms fit the model to within experimental error. However, because of the large uncertainty in the individual data points and because of the fact that the high concentration plateau was not reached, it is not possible to make a distinction between hyperbolic and other possible theoretical isotherms. The relatively large standard errors in the fitted values of k_c are a reflection of these limitations. The fitted results show that although the initial slopes of the ϵATP isotherms are very similar to those of the native nucleotides, the fitted values of k_c are a factor of ~5 larger for ϵATP reacted with S1(Mg) and S1(EDTA) than for the analogous reaction with the native nucleotides. Thus, either the first-order step is significantly faster for

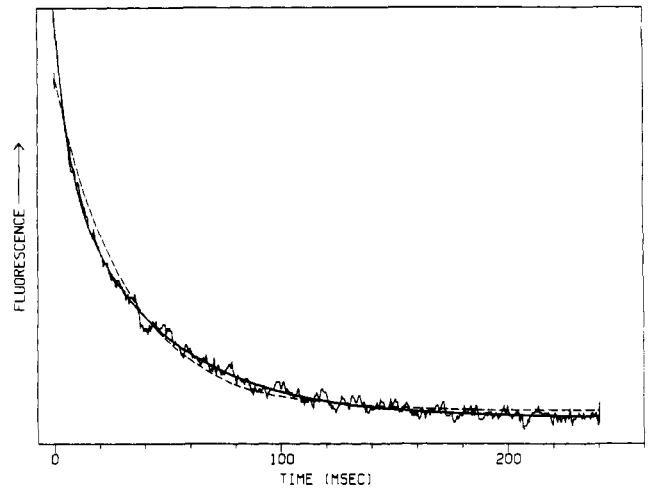

FIGURE 5: The dashed curve shows the best least-squares fit of intrinsic fluorescence change resulting from the reaction of 0.29 mM ϵADP with 10 μM S1(EDTA) to a single-exponential function (eq 1). A value of 6.8 was obtained for χ_R^2. The solid curve shows the best fit of trace to eq 2: $F(t) = 318 - 41\exp(-155t) - 72\exp(-22t)$, $\chi_R^2 = 1.2$.

fluorescent than for nonfluorescent nucleotide or a different mechanistic step is being detected with ϵATP.

The concentration dependence of k_{obsd} for the reaction of ϵADP with S1(Mg) is shown in Figure 4. k_{obsd} appears to be a linear function of [ϵADP] with a slope of 1.1×10^5 M^{-1} s^{-1}. However, traces of experiments involving nucleotide concentrations greater than ~0.3 mM did not fit eq 2 to within experimental error. Because of the low signal-to-noise ratio of these experiments, we were unable to resolve these traces into component time constants, either by deleting the initial portion of the trace or by fitting with the two-exponential function (eq 2). This suggests that the linear concentration dependence of k_{obsd} may be more apparent than real.

Biphasic traces were also obtained for the reaction of ϵADP with S1(EDTA) for nucleotide concentrations greater than 0.1 mM (see Figures 5 and 6). These traces could be fitted by eq 2 and thus resolved into a fast and a slow component, k_{obsd}^+ and k_{obsd}^-, respectively. The amplitude of the fast component ($\equiv\Delta F_{obsd}^+$, see eq 2) is relatively large at high ϵADP concentrations, but decreases with decreasing nucleotide. On the other hand, ΔF_{obsd}^- is relatively large at high and low concentrations. Below 0.1 mM nucleotide only a single rate constant having a relatively large amplitude is observed. Because of the values of k_{obsd}^+ and k_{obsd}^- and because of the concentration dependence of ΔF_{obsd}^+ and ΔF_{obsd}^-, compared with the rate and amplitude of the traces obtained below 0.1 mM ϵADP, we conclude that the single rate constant observed at low concentrations is k_{obsd}^- and that ΔF_{obsd}^+ has become

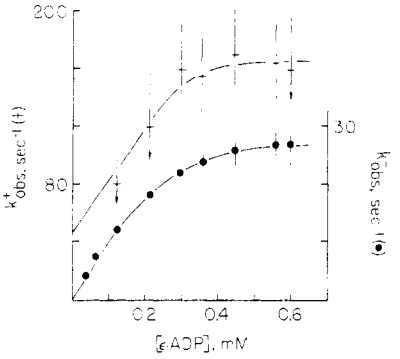

FIGURE 6: Concentration dependence of the two components, as defined by eq 2, observed for the reaction of S1(EDTA) with ϵADP. Experimental conditions are the same as those in Figure 1. Below 0.1 mM nucleotide only the slow component was observed.

vanishingly small. Although the uncertainty of k_{obsd}^+ is large, the fast component appears to level off at high nucleotide concentrations and to have a relatively large intercept; a smooth curve drawn through the data points (see Figure 6) has a limiting slope and intercept of approximately 4×10^5 M^{-1} s^{-1} and 45 s^{-1}, respectively, and levels off in the 150–200-s^{-1} range. The slow component has a well-defined limiting slope of 1.4×10^5 M^{-1} s^{-1} and levels off at 28 s^{-1}. Thus, the S1(EDTA)/ϵADP data show both a rapid first-order step, similar to that seen with ϵATP, and a slow step whose rate is virtually identical with those of the first-order steps observed with the native nucleotides. These results suggest that the binding of ϵADP to S1(EDTA) is a three-step process: the actual binding step, followed by a rapid first-order transition which in turn is followed by the previously observed (Bagshaw et al., 1974) rate-limiting isomerization.

$$M + \epsilon ADP \underset{k_{-1}}{\overset{k_1}{\rightleftharpoons}} M{\cdot}\epsilon ADP \underset{k_{-2}}{\overset{k_2}{\rightleftharpoons}} M^{\dagger}{\cdot}\epsilon ADP \underset{k_{-3}}{\overset{k_3}{\rightleftharpoons}} M^{*}{\cdot}\epsilon ADP \quad (8)$$

Computer Simulation. In order to determine whether or not the three-step mechanism given by eq 8 can quantitatively account for the S1(EDTA)/ϵADP data and also to see to what extent it is compatible with other kinetic isotherms, we carried out computer simulation "experiments". The reaction rates of the various species were calculated at 10-μs intervals by using rate equations based on the postulated mechanism. The total fluorescence signal at any time t was calculated by using $F(t) = f_i C_i$, where f_i is the emission per mole of species i and C_i is the molar concentration of i. Simulated traces were generated and fitted by eq 1 or 2, using the same nonlinear least-squares program used to fit the experimentally derived traces. Two to three milliseconds were deleted from the beginning of each trace in order to take into account instrument mixing time. An additional 5–10 ms was deleted from the traces which simulated the experiments involving native nucleotides in order that these traces would be treated by the same procedure used for the experimentally derived traces. Approximate values of the rate constants to be used in the simulation may be inferred from the binding data. First, it may be noted that the initial slopes of the ATP, ADP, and ϵATP isotherms (see Table II), as well as that of the fast component of the S1(EDTA)/ϵADP data, are quite similar, being equal to $\sim 3 \times 10^5$ M^{-1} s^{-1}. For the postulated mechanism (binding step, fast step, and slow step), the value of k_1 to be inferred from the initial slope depends on the relative values of k_{-1} and k_2 in much the same way as was true for the two-step mechanism (see above). In order for k_1 to have a value which would be reasonable for protein–ligand interactions (say $\geq 3 \times 10^6$ M^{-1} s^{-1}; Gutfreund, 1971), it is necessary that k_{-1} be a factor of at least 10 larger than k_2; i.e., the equilibrium approximation would apply to the first two steps of eq 8. This means that the values of K_b and k_c obtained by fitting the ϵATP isotherms to the hyperbola (eq 7) give K_1 and k_2 for these systems. The fact that the initial slopes of the ATP, ADP, and S1(EDTA)/ϵADP (k_{obsd}^+) isotherms are similar suggests that K_1, k_{-1}, and k_2 are approximately equal for these protein/nucleotide systems. The exact expression for the time constants of the three-step mechanism thus far described (rapid binding step; $k_{-1} \gg k_2$) may be obtained from Frost & Pearson (1961) and has been given by Johnson & Taylor (1978). Two time constants would be observed. The intercept and high concentration plateau of the fast component give k_{-2} and $k_2 + k_{-2}$, respectively, while those of the slow component give k_{-3} and $k_3 + k_{-3}$. The intercepts of the ϵATP isotherms are equal to zero, to within experimental error, while the S1(EDTA)/ϵADP data are suggestive of a relatively large intercept ($\simeq 45$ s^{-1}) for the fast step. The values of k_{-2} inferred from these intercepts are consistent with the concentration dependence of the amplitudes of the fast time constant. For both S1(Mg)/ϵATP and S1(EDTA)/ϵATP the amplitudes are relatively large and constant (per protein binding site; corrected for nucleotide absorption at the excitation wavelength) down to the lowest nucleotide concentrations used (20 μM). This suggests that the equilibrium constants of the first two steps are sufficiently high so that all, or nearly all, protein is converted from M to $M^{\dagger}{\cdot}\epsilon ATP$ by steps 1 and 2 alone, even at 20 μM substrate, and thus requires [provided $K_1 = (1–2) \times 10^3$ M^{-1} and $k_2 = 200$ s^{-1}, as concluded above] that $K_2 \geq 1 \times 10^3$ and hence that $k_{-2} \leq 0.2$ s^{-1} for ϵATP + protein. On the other hand, the amplitude of the S1(EDTA)/ϵADP fast component decreases with decreasing [ϵADP], disappearing entirely below ~0.1 mM ligand. Since the $M{\cdot}\epsilon ADP$ to $M^{\dagger}{\cdot}\epsilon ADP$ transition involves a signal change, the disappearance of the fast component at low ligand concentrations must occur because the combined binding constant of the first two steps, K_1K_2, is too low for a significant amount of ϵADP to be bound during the rapid phase. If K_1 is taken to be $(1–2) \times 10^3$ M^{-1}, this behavior requires that K_2 be of the order of magnitude of 1.0 for S1(EDTA) + ϵADP. Estimates of k_3 and k_{-3} may be obtained from S1(EDTA)/ϵADP (k_{obsd}^-), ATP, and ADP isotherms. Since high concentration plateaus of ~35 s^{-1} are obtained for all of these systems, $k_3 + k_{-3} = 35$ s^{-1}. The intercept of the slow component of S1(EDTA)/ϵADP is zero to within experimental error. In addition, the rate of dissociation of ϵADP from S1(EDTA) was measured to be 0.20 s^{-1} (see Table I). If both k_{-1} and k_{-2} are relatively large, as concluded above, then k_{-3} must equal 0.20 s^{-1}.

S1(EDTA)/ϵADP traces were simulated on the basis of the mechanism given by eq 8, using the procedure given above. The values of k_1 and k_{-1} used in the simulation were 4×10^6 M^{-1} s^{-1} and 2000 s^{-1}. It was found, as expected since k_1, $k_{-1} \gg k_2$, that k_1 and k_{-1} could be varied over a fairly wide range without affecting the resulting trace. However, the ratio k_1/k_{-1} ($=K_1$) did have some effect on the observed rate constants, particularly k_{obsd}^+, obtained from the fitted trace. k_2, k_{-2}, and k_3 were varied in order to obtain a set of values of the rate constants producing synthetic k_{obsd}^+ and k_{obsd}^- isotherms which agreed with the measured isotherms to within the experimental error of the latter. The range over which these rate constants were varied was as follows: k_2, 50–250 s^{-1}; k_{-2}, 0–150 s^{-1}; k_3, 25–50 s^{-1}. k_{-3} was set equal to 0.20 s^{-1}. It was found that $k_2 = 200$ s^{-1}, $k_{-2} = 45$ s^{-1}, and $k_3 = 35$ s^{-1} fulfilled the above criterion. Changing these values by more than ~20% pro-

duced significant differences between synthetic and experimental isotherms; k_2 affected the high concentration plateau of k_{obsd}^+ while the initial slope and plateau of the calculated k_{obsd}^- isotherm were strongly dependent on the ratio k_{-2}/k_3 and on k_3, respectively. It is noteworthy that the values of k_2 and k_3 are quite similar to the values of these rate constants obtained from the ϵATP and native nucleotide isotherms, respectively, and that $k_{-2} = 45\ s^{-1}$ is in excellent agreement with the result inferred from the k_{obsd}^+ isotherm. It was also found that the values of $\Delta F^+/\Delta F^-$ obtained from the simulated traces were in good agreement with the experimental values if $f_{M^\dagger\cdot\epsilon ADP} = f_{M^*\cdot\epsilon ADP}$. This result suggests that for ϵADP as well as ϵATP, the intensity of fluorescence emission of $M^\dagger\cdot X$ is similar if not equal to that of $M^*\cdot X$. It is clear from the simulation calculation that step 3 is seen for the S1-(EDTA)/ϵADP system only because the combined equilibrium constant of the first two steps is sufficiently low so that only part of the protein is bound during the fast phase. The remainder of the protein is bound during the slow phase, the amplitude of which is nonetheless due to steps 1 and 2.

In order for the three-step scheme postulated above to account for the binding of the native nucleotides to myosin S1, it is necessary that the observed signal change originate at least primarily from the $M^\dagger\cdot$ATP to $M^*\cdot$ATP (or $M^\dagger\cdot$ADP to $M^*\cdot$ADP) step rather than from step 2. If only step 3 involves a signal change, then relatively large phase lags should be observed. This may be seen by simulating the S1(Mg)/ATP isotherm, using $k_1 = 4 \times 10^6\ M^{-1}\ s^{-1}$, $k_{-1} = 2000\ s^{-1}$, $k_2 = 200\ s^{-1}$, $k_{-2} = 0.1\ s^{-1}$, $k_3 = 40\ s^{-1}$, $k_{-3} = 0.1\ s^{-1}$, $f_M = f_{M\cdot ATP} = f_{M^\dagger\cdot ATP} = 1.0$, and $f_{M^*\cdot ATP} = 1.5$. Even with the first 10–13 ms deleted, the simulated traces deviated somewhat from a single-exponential function. More strikingly, the fitted values of k_{obsd} obtained from these traces were significantly lower than those obtained experimentally. For example, at [ATP] = 0.20 mM, the simulated rate of fluorescence enhancement was 21 s^{-1} compared with 32 s^{-1} actually observed. The S1(Mg)/ATP isotherm could be reproduced, to within experimental error, by increasing the value of k_2 used in the simulation. It was found that $k_2 = 600\ s^{-1}$ gave acceptable phase lag and k_{obsd} results. This would suggest that step 2 is significantly faster for native than analogue nucleotide. However, it was also found that lower values of k_2 could also produce acceptable isotherms, providing the M·ATP to $M^\dagger\cdot$ATP transition involved some signal change. For example, if $f_M = f_{M\cdot ATP} = 1.0$, $f_{M^\dagger\cdot ATP} = 1.1$, and $f_{M^*\cdot ATP} = 1.5$, then $k_2 = 350\ s^{-1}$, a value nearly equal to that obtained experimentally, reproduced the isotherm satisfactorily. Thus, the native nucleotide data are consistent with the three-step mechanism given by eq 8, with the proviso that step 2 is at least slightly faster for native than for analogue nucleotide and probably involves some enhancement of intrinsic fluorescence.

Discussion

The kinetics of the binding of substrate and product nucleotides to myosin subfragment 1 has been investigated by monitoring the protein tryptophan fluorescence as either ATP, ϵATP, ADP, or ϵADP binds to S1. Neither the native nor analogue data can be satisfactorily explained by the two-step mechanism originally proposed by Bagshaw et al. (1974). The experimental results, particularly the S1(EDTA)/ϵADP data, indicate that a minimum of three elementary steps is needed to describe nucleotide binding. The three-step mechanism given by eq 8 represents a simple extension of the two-step model originally proposed by Bagshaw et al. (1974) and, as discussed under the Computer Simulation section, is compatible with both native and analogue results. The mechanism is postulated to consist of (1) a binding step, characterized by rapid kinetics and a low equilibrium constant [$K_1 = (1\text{–}2) \times 10^3\ M^{-1}$], (2) a rapid first-order transition having a reasonably large equilibrium constant for substrate but a very small constant for product nucleotides, and (3) a relatively slow first-order step, initially observed for native nucleotides by Bagshaw et al. (1974). This mechanism gives biphasic stopped-flow traces: a rapid phase, due to steps 1 and 2, and a slow phase, due to step 3. The experimental results would require that step 1 or step 2, or both, involves significant quenching of tryptophan fluorescence when S1 is reacted with ϵ nucleotides but that the emission of M, M·X, and $M^\dagger\cdot X$ is similar when X ≡ ATP or ADP. As noted above, step 2 (or step1) could involve some degree of fluorescence enhancement in the case of the native nucleotides. On the other hand, our results indicate that the tryptophan emissions of $M^\dagger\cdot X$ and $M^*\cdot X$, the complexes involved in step 3, are nearly equal for X ≡ ϵATP or ϵADP. This would suggest that, unlike the native nucleotides, the analogues do not induce enhancement of tryptophan fluorescence upon binding. Alternatively, tryptophan enhancement may occur but be canceled by quenching due to energy transfer from intrinsic fluorophores to ϵ nucleotide occurring during the same step. Onishi et al. (1973) have concluded, on the basis of iodide quenching experiments, that (1) the binding of ϵATP to heavy meromyosin results in enhanced tryptophan emission, the actual increase in fluorescence being 80% of that of the native substrate both in the presence and absence of iodide, and (2) the residues involved in the tryptophan → ϵATP energy-transfer process remain exposed (i.e., accessible to iodide quenching) during binding and are therefore not the same residues whose fluorescence is enhanced. This result suggests that the second of the above two possibilities is correct: that step 3 is not seen with ϵATP because of the fortuitous canceling of the enhancement and quenching processes.

The ϵ-nucleotide data provide information on the magnitudes of the equilibrium constants of the first two steps. Our data suggest that K_1 is relatively independent of the nucleotide or protein studied. As seen above, K_1 is similar for ϵATP or ATP reacting with intact protein. The results obtained from fitting eq 7 to the ϵATP isotherms show that K_1 is only a factor of ~2 larger for light chain deficient protein than for intact protein. It is interesting, in this respect, that a recent spectrofluorometric study of the binding of ϵADP to both proteins shows that the overall binding constant of S1(EDTA)/ϵADP is approximately twice that of S1(Mg)/ϵADP: 4.5×10^5 vs. $1.8 \times 10^5\ M^{-1}$ (F. Garland and H. C. Cheung, unpublished experiments). A smaller value of K_1 could account for our inability to resolve the high concentration S1(Mg)/ϵADP traces into fast and slow components. If K_1 for S1(Mg)/ϵADP were half that for S1(EDTA)/ϵADP, it would be necessary to have approximately twice the nucleotide concentration in order to bind sufficient protein to observe k_{obsd}^+, providing the values of K_2 and the f_i are similar for the two systems. In fact, evidence of biphasicity does occur at ~0.3 mM ϵADP for S1(Mg) as opposed to 0.12 mM nucleotide for S1(EDTA). The smaller limiting slope of S1(Mg)/ϵADP would also tend to increase the nucleotide concentration at which biphasic traces would be observed. Since the ϵ nucleotides absorb at 295 nm, the signal-to-noise ratio of the experiments decreases with increasing [ϵADP], and with it our capability of resolving multicomponent traces.

In contrast with the binding step, K_2 seems strongly dependent on the nucleotide used in the reaction. The results indicate that K_2 is quite large (10^3 or greater) for S1(Mg)/

ϵATP and probably S1(Mg)/ATP also but rather small for S1(EDTA)/ϵADP and S1(Mg)/ϵADP (in the range of 1–4). The large differences in K_2 are due primarily to changes in k_{-2} since k_2 is roughly (within a factor of 2 to 3) equal for the ϵ-nucleotide systems. If k_2 is similar for the ADP and ϵADP systems, then the fact that the limiting slopes of the ADP isotherms are twice those of the ϵADP isotherms would suggest that k_{-2} is a factor of $\sim$10 lower, and K_2 proportionately higher, for ADP than for ϵADP. The very rapid rate of step 2, together with the large equilibrium constant of this step observed with substrate and the small value observed with product, suggests that this step may be directly involved in the actin dissociation step. This is supported by the stopped-flow–light-scattering experiments of Sleep & Taylor (1976), from which it was determined that the actin dissociation step is considerably faster than the fluorescence enhancement step and also that the rate of fluorescence enhancement is the same for S1 and for acto-S1. Thus, the first dissociated state in the acto-S1 ATPase pathway must be a complex formed prior to M*·ATP. It was also concluded, on the basis of phosphate burst experiments using ^{32}P-labeled ATP, that substrate is not freely exchangeable from the first dissociated state. This suggests that M†·ATP and not M·ATP could be the complex resulting from actin dissociation.

$$\text{A·M} + \text{ATP} \rightleftharpoons \text{A·M·ATP} \rightleftharpoons \underset{\text{A}}{\text{M}^{\dagger}\cdot\text{ATP}} \rightleftharpoons \text{M*·ATP} \rightleftharpoons$$

A represents actin. The existence of M†·ATP in the S1 ATPase pathway should result in a biphasic trace being obtained from binding experiments involving the association of the native substrate with the myosin active site. As noted above, both the ATP and ADP results are suggestive of biphasicity. Biphasic traces have been reported by Johnson & Taylor (1978) and Trybus & Taylor (1979).

The kinetic results show that the high concentration rates of the first-order process observed with the native nucleotides (see Figures 1 and 2) and those observed with the analogues (Figures 3, 4, and 6) are significantly affected by removal of the DTNB light chain. In terms of the three-step mechanism given by eq 8, this result suggests that the possible conformational changes represented by steps 2 and 3 involve the light chain to some extent. In view of (a) the finding that the DTNB light chain affects the myosin–actin interaction both in the presence and absence of ATP (Margossian et al., 1975; Hozumi & Hotta, 1978) and (b) the significant effect of the light chain on the formation of M†·ϵATP seen above, it seems likely that comparative transient kinetic studies on the interaction of ϵATP with acto-S1(EDTA) vs. acto-S1(Mg) would help elucidate the role of the light chain in the contractile process.

Bagshaw et al. (1974) concluded that the fluorescence enhancement step, observed with the native nucleotides and with the slowly hydrolyzable substrate analogue adenosine 5′-(3-thiotriphosphate), represents a conformation change for both substrate and product nucleotides and that the conformation change of the S1/ATP complex is immediately followed by the cleavage step. Since the cleavage step is also thought to involve enhancement of tryptophan fluorescence and yet was not seen as a separate phase, it was suggested that hydrolysis must proceed considerably faster than the preceeding conformation change. Johnson & Taylor (1978) reinvestigated the binding of ATP to S1 and concluded that substrate binds to protein according to a three-step mechanism which is formally very similar to that postulated above. As above, step 3 is the fluorescence enhancement step originally observed by Bagshaw et al. (1974). On the basis of various data, including the ionic strength dependence of the rate constants, it was concluded that this step is the cleavage step itself. From the results of this work, it may be seen that the rate of the fluorescence enhancement step is approximately equal for ATP and ADP and furthermore that removal of the DTNB light chain decreases the rate of this step for both nucleotides to a similar degree. In addition, the S1(EDTA)/ϵADP data show a first-order step, the rate of which is identical with that of the enhancement step found for S1(EDTA)/ADP. Finally, it may now be seen that the temperature dependence of the rate of the enhancement step is the same for ATP as for ADP, both at pH 7 and at pH 8 (Johnson & Taylor, 1978; Trybus & Taylor, 1979; Bagshaw et al., 1974; this work). These findings lend support to the original conclusion of Bagshaw et al. (1974) as to the physical significance of this step. For substrate, it was postulated (Bagshaw & Trentham, 1974) that this step is followed by the actual hydrolysis step.

$$\ldots\text{M}^{\dagger}\cdot\text{ATP} \underset{k_{-3}}{\overset{k_3}{\rightleftharpoons}} \text{M*·ATP} \underset{k_{-4}}{\overset{k_4}{\rightleftharpoons}} \text{M**·ADP·P}_i\ldots \qquad (9)$$

Since it is generally agreed that the cleavage step also involves a change in intrinsic protein fluorescence and since no fluorescence transitions following step 3 are observed, it is of interest to see what constraints are placed on the rate and relative fluorescence change of step 4. This may be done by obtaining simulated traces based on the four-step reaction mechanism given by eq 8 and 9. The rate constants of the first three steps used in this calculation had the same values used above to satisfactorily reproduce the S1(Mg)/ATP isotherm, although the results do not depend on this condition. The concentration of ATP used was 1.0 mM so that if only the first three steps were used to obtain simulated traces, $k_{obsd} = k_3 + k_{-3} = 40$ s^{-1}. The results show that if the relative fluorescence changes of steps 3 and 4 are equal, e.g., $f_{M^{\dagger}\cdot ATP} = 1.0$, $f_{M^{*}\cdot ATP} = 1.25$, and $f_{M^{**}\cdot ADP\cdot P_i} = 1.5$, $k_4 + k_{-4} = 100$ s^{-1} gives $k_{obsd} = 37$ s^{-1} with slight deviation from single exponential decay at the beginning of the trace. Decreasing the relative fluorescence change of the cleavage step (4) with respect to that of step 3 results in lower values of $k_4 + k_{-4}$ satisfactorily reproducing experimental traces. For example, if $f_{M^{\dagger}\cdot ATP} = 1.0$, $f_{M^{*}\cdot ATP} = 1.4$, and $f_{M^{**}\cdot ADP\cdot P_i} = 1.5$, then $k_4 + k_{-4} = 50$ s^{-1} gave $k_{obsd} = 36$ s^{-1} with the trace fitting a single exponential to within the experimental error of our instrument. These results show that the experimental data are consistent with a cleavage step whose rate could be as small as twice that of the preceeding conformation change step and might, depending on the relative fluorescence changes involved, be nearly as slow as the cleavage step. The experimental and computer results presented above do not consitute definitive proof concerning the molecular basis of the observed fluorescence enhancement step. We consider that such proof is still lacking and requires additional studies.

Added in Proof

Subsequent to the submission of this paper, Trybus & Taylor (1979) reported at the Biophysical Society Meeting that biphasic traces were resolved for the binding of ADP and AMP-PNP (5′-adenylyl imidodiphosphate) to myosin subfragment 1 at 3 and 20 °C, respectively. These results led them to postulate a three-step binding mechanism involving two fluorescence transitions with $k_2 > k_3$. These results are in qualitative agreement with those reported here for the binding of nonhydrolyzable nucleotides to myosin S1.

Acknowledgments

The authors thank Susan Yarborough for excellent labora-

tory assistance and the Josiah Macy, Jr., Research Computer Center, under the direction of Michael P. White, for invaluable assistance in the data acquisition aspects of this work.

References

Bagshaw, C. R., & Trentham, D. R. (1974) *Biochem. J. 141*, 331.
Bagshaw, C. R., & Reed, G. H. (1977) *FEBS Lett. 81*, 386.
Bagshaw, C. R., Eccleston, J. F., Eckstein, F., Goody, R. S., Gutfreund, H., & Trentham, D. R. (1974) *Biochem. J. 141*, 351.
Frost, A. A., & Pearson, R. G. (1961) *Kinetics and Mechanisms*, p 162, Wiley, New York.
Garland, F., & Cheung, H. C. (1976) *FEBS Lett. 66*, 198.
Garland, F., & Cheung, H. C. (1978) *Biophys. J. 21*, 218a.
Gutfreund, H. (1971) *Annu. Rev. Biochem. 40*, 315.
Hozumi, T., & Hotta, K. (1978) *J. Biochem. (Tokyo) 83*, 671.
Huxley, H. E. (1969) *Science 164*, 1356.
Johnson, K. A., & Taylor, E. W. (1978) *Biochemistry 17*, 3432.
Lymn, R. W., & Taylor, E. W. (1971) *Biochemistry 10*, 4617.
Margossian, S. S., Lowey, S., & Barshop, B. (1975) *Nature (London) 258*, 163.
Marquardt, D. W. (1963) *J. Soc. Ind. Appl. Math. 11*, 431.
Marsh, D. J., d'Albis, A., & Gratzer, W. (1978) *Eur J. Biochem. 82*, 219.
Onishi, H., Ohtsuka, E., Ikehara, M., & Tonomura, Y. (1973) *J. Biochem. (Tokyo) 74*, 435.
Sleep, J. A., & Taylor, E. W. (1976) *Biochemistry 15*, 5813.
Taylor, R. S., & Weeds, A. G. (1977) *FEBS Lett. 75*, 55.
Tonomura, Y., Appel, P., & Morales, M. F. (1966) *Biochemistry 5*, 515.
Trybus, K. M., & Taylor, E. W. (1979) *Biophys. J. 25*, 21a.
Werber, M. M., & Oplatka, A. (1974) *Biochem. Biophys. Res. Commun. 57*, 823.
Werber, M. M., Szent-Györgyi, A. G., & Fasman, G. D. (1972) *Biochemistry 11*, 2872.

Unequal Gene Amplification and Transcription in the Macronucleus of *Tetrahymena pyriformis*†

Yukio Iwamura,‡ Masaharu Sakai, Takashi Mita,§ and Masami Muramatsu*

ABSTRACT: Deoxyribonucleic acid (DNA) repetition classes of the micro- and macronuclei of *Tetrahymena pyriformis* were analyzed by reassociation kinetics. The most slowly reassociating class of DNA, which accounted for ~80% of the total micronuclear DNA, had a $C_0t_{1/2}$ value of ~200. This value corresponds well to that for the single-copy (nonrepetitive) sequences with a genome size of 0.4 pg of DNA per diploid micronucleus. There were other sequences reannealing a hundred times or several hundred times faster, each constituting ~10% of the micronuclear DNA. They are assumed to represent moderately and highly repeated sequences in this genome. On the other hand, macronuclear DNA was composed of nearly only one repetitive class whose $C_0t_{1/2}$ value was 200, similar to the value for the single-copy class DNA of the micronucleus. This indicates that most, if not all, of the macronuclear DNA exists as rather uniformly repeated sequences with a frequency equal to the DNA ratio of macro-/micronucleus. This ratio has been reported to be 23 (Doerder et al., 1977; Williams et al., 1978). We conclude from these results that, when a macronucleus develops from the micronucleus, the single-copy sequences amplify by more than 20 times, while the repeated sequences remain virtually unamplified or amplify to a much lesser extent, a few times at most. Hybridization experiments with DNA complementary to poly(A)-containing ribonucleic acid (RNA) and micro- or macronuclear DNA indicate that, although all three classes of DNA in the micronuclear genome are transcribed into messenger ribonucleic acid (mRNA), the sequences transcribed from moderately repeated DNA accounting for only a few percent of the macronuclear DNA make up more than 30% of the mRNA, suggesting the higher production and/or stability of these sequences.

The ciliated protozoan *Tetrahymena pyriformis* possesses a transcriptionally inactive, diploid, germinal micronucleus and a transcriptionally active, polyploid, somatic macronucleus. In vegetatively growing cells, the micronucleus divides mitotically, whereas the macronucleus divides amitotically. During the course of sexual conjugation, the macronucleus is destroyed and then resorbed, while the micronucleus undergoes meiosis. After subsequent reciprocal exchange and fusion of the two haploid genetic nuclei, a new macronucleus develops through a process of amplification of micronuclear DNA to ~45-ploid (Woodard et al., 1972; Doerder et al., 1977). The multiple copies of rRNA genes in the macronucleus are generated by amplification of the apparently single gene in the micronucleus (Yao & Gall, 1977), reaching a higher multiplicity than other DNA sequences (Yao et al., 1974). On the contrary, renaturation kinetics of macro- and micronuclear DNA were reported to be very similar, suggesting that no significant unproportional gene amplification occurred on the extranucleolar genomic DNA except that some 10–20% of the micronuclear DNA sequences appeared to be absent in macronuclear DNA (Yao & Gorovsky, 1974).

We reexamined the reassociation kinetics of these DNAs with our highly purified micro- and macronuclear preparations and with the aid of highly labeled DNA markers prepared by the nick translation technique which had been developed by Rigby et al. (1977). The results obtained indicate that the

† From the Department of Biochemistry, Cancer Institute, Japanese Foundation for Cancer Research, Kami-ikebukuro, Toshima-ku, Tokyo, Japan. *Received May 22, 1979.* Supported in part by grants from the Ministry of Education, Science and Culture, and from the Ministry of Labor, Japan.

‡ Present address: Department of Microbiology, Institute of Basic Medical Science, Tsukuba University, Ibaragi, Japan.

§ Present address: Department of Molecular Biology, School of Medicine, University of Occupational and Environmental Health, Kita-Kyushu, Japan.

0006-2960/79/0418-5289$01.00/0